Demonstration of a method to construct self-consistent beam distributions through phase space painting (DRAFT)

Nicholas J. Evans[†],[*] Austin Hoover,[†] Timofey Gorlov, and Vasiliy Morozov
Oak Ridge National Laboratory, Oak Ridge, Tennessee 37830, USA
(Dated: May 6, 2025)

Multi-turn charge-exchange injection is the primary method of creating high-intensity hadron beams in circular accelerators. Phase space painting during injection enables tailoring of the accumulated phase-space distribution. For the first time, we implement a technique called *eigenpainting* to uniformly inject beam into a single non-planar mode of a coupled ring. Under ideal conditions uniform eigenpainting generates an equilibrium distribution with uniform density in the transverse real-space projection, an elliptical envelope and linear space charge, which can be injected self-consistently. We demonstrate injection into a one non-planar mode in the Spallation Neutron Source Accumulator Ring. We demonstrate sufficient control over injection of the centroid of a single bunch into one mode with emittance ratio ≈80. For multi-turn injection of 8.8 μC of 800 MeV beam we obtain an emittance ratio of ≈2.4.

Introduction—In high-intensity hadron rings that accumulate beam through multi-turn injection, phase space painting, or painting, provides control of beam distributions through control of the relative position and angle of circulating and injected beam [1]. To date, experimental exploration of novel injection schemes has been limited by the lack of flexibility in injection systems and optics in rings equipped for multi-turn injection. *Eigenpainting* can be used to uniformly fill one non-planar mode of a coupled ring lattice [2]. Uniform eigenpainting generates a special case of the well-known Kapchinskij-Vladimirskij (KV) [3] distribution that is stationary throughout injection. We call this special case the Danilov distribution. Interest in the Danilov distribution is based on its relationship to both the KV distribution, and to circular modes. The uniform charge distribution, and vanishing 4D emittance have important implications for the control of space charge effects, and applications in colliders [4]. Control of space charge effects is one of the main challenges for high-intensity hadron accelerators, for which there exists a number of novel proposals [5], [6]. In this Letter, we report on the first experimental demonstration of the eigenpainting method.

The KV distribution is the only known, equilibrium solution of the Vlasov-Poisson equations in time-dependent, linear focusing systems. The KV distribution has long been a staple of accelerator design studies and theoretical exploration and remains an area of active research [7], [8]. The KV distribution is essentially a microcanonical ensemble in transverse invariants of motion originally proposed to explore the limits of space charge in high-intensity rings as it linearizes space charge force. The phase space density ρ in the KV distribution is given by,

$$\rho(J_1, J_2) \propto \delta(1 - (J_1/\tilde{J}_1 + J_2/\tilde{J}_2)), \qquad (1)$$

where $J_{1,2}$ and $\tilde{J}_{1,2}$ are the transverse actions and their maximal values, respectively, and δ is the Dirac delta function. The KV distribution features a hard-edged, elliptical envelope with uniform charge density in any 2-D projection, leading to linear space charge forces. This minimizes tune spread, a limiting factor for beam intensity in rings, by providing a uniform tune shift across the beam. Crosbie [9] proposed a painting scheme that would result in a KV, but the distribution is not stationary during injection. The experimental realization of a KV distribution painted self-consistently in the presence of significant space charge would allow experimental validation of models of stability [10], halo-formation, and design principles developed over decades.

In the limit $\tilde{J}_2 \to 0$ particles occupy a single mode and the distribution of particles in 4D phase space, ρ, becomes

$$\rho(J_1, J_2) \propto \Theta(J_1)\delta(J_2), \qquad (2)$$

where Θ is the Heaviside step function and we take mode 1 to be the mode with non-zero amplitude for simplicity. Because the amplitude of J_2 vanishes, the invariant 4D volume, or emittance, $\varepsilon = \varepsilon_1\varepsilon_2 \propto \langle J_1\rangle\langle J_2\rangle$, tends to zero. This special case is identical to the Danilov distribution [11], which can be expressed as a single uniformly filled mode.

In an uncoupled system, modes are described as flat (planar), since motion in each planar mode appears as a line along the corresponding axis in the x-y plane. Coupling can transform planar modes into non-planar, or elliptical, modes. In general, each mode is a 2D ellipse in 4D space which projects onto the x-y plane as an ellipse [12]. Each non-planar mode is characterized by non-zero angular momentum of opposite sign due to correlated motion in $x - y'$ and $y - x'$.

Unlike planar beams, beams with non-zero angular momentum have radially separated elliptical trajectories in real space. Further, the space charge force in a uniformly populated mode is linear, and proportional to the beam density. Danilov recognized that once the beam core is established, rotational trajectories imply that additional

[*] nhe@ornl.gov
[†] These authors contributed equally to this work.

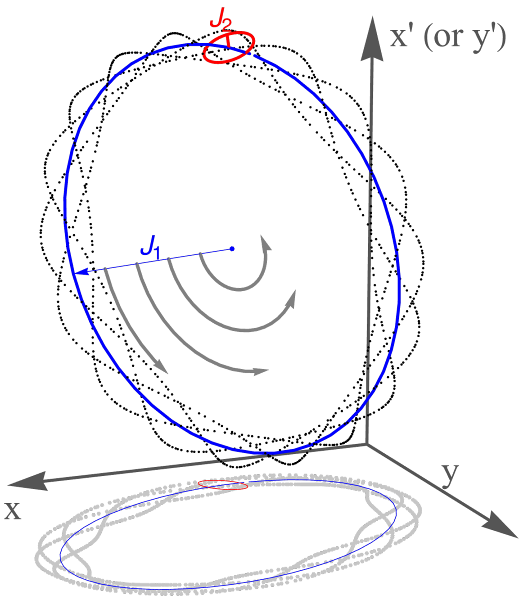

FIG. 1. Projection of 4D phase space trajectory onto 2- and 3D shown as gray dots. The blue ellipse represents mode 1, red mode 2. The painting trajectory should follow the blue arrow.

beam can be added at larger radii maintaining a stationary distribution ideal for phase space painting. Achieving non-planar modes in a standard, strong-focusing lattice requires special optics not typically available in machines equipped for phase space painting. We achieve non-planar modes in the SNS using a scheme based on Danilov's proposal and subsequent simulations [13]. The betatron tunes are first set equal in an uncoupled lattice resulting in a coupling resonance with degenerate eigenmodes. A solenoid breaks the degeneracy of motion establishing two unique non-planar modes.

In addition to accommodating painting, non-planar modes have other attractive features for high-intensity machines. Notably, space charge tune shift depends on the transverse beam size, and for beams prepared in circular modes, the beam size is determined by the larger emittance. The other mode's emittance can be arbitrarily small, allowing for a brighter beam for a given tune shift regardless of charge uniformity [14]. The implications of a beam which is both non-planar and KV have been discussed by several authors, including space charge tune shift reduction [4], extreme cooling of one mode [15], instability suppression [16], and intrabeam scattering [17].

Electron beams in non-planar modes, also known as magnetized beams [18], are an active area of research that have been studied extensively and successfully applied in hadron cooling applications [19]. Flat beams, magnetized beams transformed to occupy one planar mode, have also been produced at the the Relativistic Heavy-Ion Collider through cooling [20]. To our knowledge the experiment reported on in this manuscript is the first to create beam in an elliptical mode through phase space painting, which allows the additional freedom to distribute the beam uniformly in the $x-y$ plane.

As a single uniformly-filled, non-planar mode, the quality of the painted distribution is characterized by the following observable features: (i) uniform charge density (ii) elliptical envelope (iii) low intrinsic 4D emittance. We measure these properties to demonstrate successful eigenpainting into the Spallation Neutron Source (SNS) ring. We will proceed from a description of phase space painting to the particular procedure used at the SNS and a discussion of the experiment.

Phase Space Painting—During painting, beam injected at time t has centroid coordinates $\mathbf{x}(t)$ relative to the closed orbit of the ring in the 4D phase space. The trajectory determines the distribution that will be painted. This trajectory can be expressed in action-angle coordinates (J, Ψ) of the normal modes of the single-turn transfer matrix:

$$\mathbf{x}(t) = \Re\left\{\sqrt{J_1(t)}\mathbf{v}_1 e^{-i\Psi_1(t)} + \sqrt{J_2(t)}\mathbf{v}_2 e^{-i\Psi_2(t)}\right\}, \quad (3)$$

where $\mathbf{v}_{1,2}$ are the eigenvectors of the 4×4 transfer matrix $\mathbf{M}$, normalized according to the Bogacz-Lebedev convention [12].

The two most common schemes are *correlated* and *anti-correlated* painting [21], [9], [22], which have historically been considered in the uncoupled case. We extend their standard definitions by generalizing the uncoupled modes, $J_{x,y}$, to $J_{1,2}$. In correlated painting, both J_1 and J_2 increase from a minimum value, J_{0k}, to $\tilde{J}_k$, with $k = 1, 2$, while in anti-correlated painting J_1 increases while J_2 decreases[23]. In the absence of space charge anti-correlated painting leads to the KV distribution [9]. In the presence of space charge, both schemes produce non-stationary distributions during injection, the effects of which can impact beam quality [24]. Figure 2 shows beam in the *x*-*y* during accumulation, and the trajectory in terms of J's to realize these schemes.

We define *eigenpainting* as the limit of either correlated or anti-correlated painting as either of the two amplitudes $\tilde{J}_k \to 0$. We let J_2 vanish without loss of generality. When $J_1(t) = \tilde{J}_1 t/T$, the mode is uniformly filled and the beam injected approaches the Danilov distribution.

Each mode is described by a complex eigenvector that sweeps out a 2D elliptical path in 4D phase space [12]. To paint into a single mode, the painting trajectory in 4D phase space, $\mathbf{x}(t)$, must lie in the plane of the eigenvector. We hold the phase constant throughout, painting along a line in 4D space which begins at the closed orbit at time $t = 0$. The action increases linearly to a maximum action, J_{max}, at time $t = T$ to uniformly fill the mode. This is depicted in three dimensions in Fig. 1 by the blue arrow. Action is proportional to amplitude squared, so the trajectory of the closed orbit can be written,

$$\mathbf{x}_{co}(t) = \sqrt{t/T}\ \Re\{\mathbf{v}_1 e^{-i\Psi_1}\}, \quad (4)$$

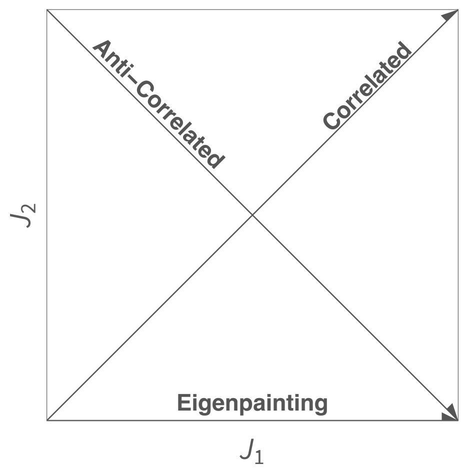

(a) Schematic trajectories for several painting schemes.

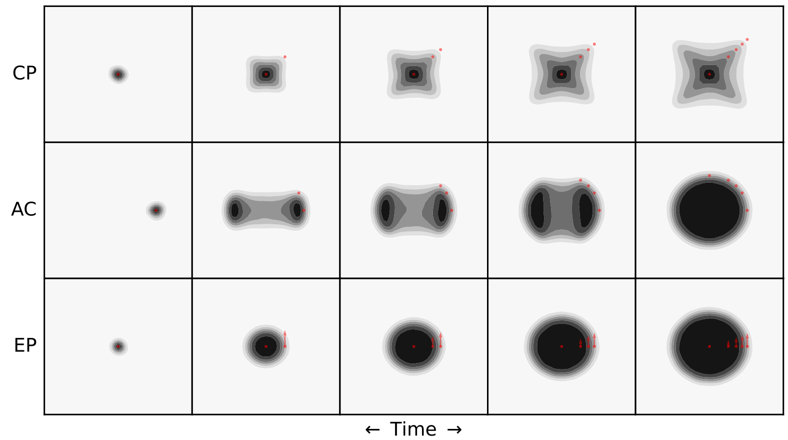

(b) x-y distributions.

FIG. 2. Representation of the painting trajectories in the plane of mode actions, $J_{1,2}$ corresponding to correlated (CP), anti-correlated (AP) and eigenpainting (EP) schemes and time evolution of the x-y distribution of beam produced by the corresponding schemes. Red points indicate the centroid position of injected beamlets, arrows indicate centroid angle if non-zero.

where $0 \leq t \leq T$. By varying the injection time T at a constant injection rate from the linac, the same beam size can be painted with higher density. For dense enough beams space charge modifies the matched solution. Accounting for the linear space charge, the matched solution can be expressed as a modified eigenvector in the same linear formulation [25][26].

Experimental Demonstration—We performed an experiment to demonstrate eigenpainting in the Spallation Neutron Source (SNS) at Oak Ridge National Laboratory. The SNS consists of a 1.3 GeV superconducting H^- linac, a 248 m long Accumulator Ring, and a transport line to the liquid mercury target. The ring injection system is one of the most flexible in the world, providing time-varying control of the position and angle of the closed orbit at the injection location throughout the 1 ms injection cycle. To increase the reach of the injection system, these experiments were conducted at a kinetic energy of 800 MeV. For the final painting, we injected 8.8 μC beam over 600 turns (588 μs). The Ring-Target Beam Transport (RTBT) line is equipped with wirescanners and sufficiently flexible optics to reconstruct the 4D distribution of the bunch extracted from the ring.

Defining the painting trajectory requires finding the amplitude settings for the eight injection kickers, $\mathbf{K}$, that correspond to the initial and final points on the trajectory Eq. 4: $\mathbf{x}(0) \to \mathbf{K}_0$ and $\mathbf{x}(T) \to \mathbf{K}_T$. We use standard techniques for analysing turn-by-turn BPM data and a calibrated linear model of the ring to find the injection coordinates corresponding to kicker amplitudes, $\mathbf{K}$.

The tunes of the uncoupled ring are initially set to $\nu_x = \nu_y = 0.177$. Powering on the solenoids we measure $\nu_1 = 0.196$, $\nu_2 = 0.158$, a tune split of $\Delta\nu = 0.037$. Figure 3a shows vertical and horizontal turn-by-turn data for one $\approx$ 10 nC pulse of beam at one BPM used for tune calibration. Coupling is evident in the modulation of the envelope due to beating between ν_1 and ν_2 present in both planes. We choose one mode for injection, and a phase that minimizes the horizontal angle to minimize losses caused by the geometry of apertures near the injection region [13].

To find the amplitude of each mode, we extend Pelaia's [27] analysis of the damped beam centroid to the modes of a coupled ring. Assuming Gaussian energy spread in the presence of chromaticity, the 4D coordinates of the bunch centroid, $\mathbf{x}$, evolve according to

$$\mathbf{x}^j(n) = \sum_{k=1,2} A_k e^{-(\gamma_1 n^2 + i2\pi(n\nu_k + \Psi_k))} \mathbf{v}_k^j(n) + \mathbf{c}^j, \quad (5)$$

where n is the turn number, k is mode number, j is the BPM index, and $\mathbf{c}$ is the closed orbit offset in the BPM. Ψ_k and A_k are the injection phase and amplitude of the bunch in each mode. ν_k and γ_k are the tunes and damping coefficients, respectively, for each mode. ν_k and γ_k are global parameters fit geometrically using data containing both modes to calibrate the ring optics. The complex eigenvectors, $\mathbf{v}^j$, are then extracted from a linear model calibrated to the observed tunes. The injection specific parameters, A_k, Ψ_k, $\mathbf{c}$ are fit globally for each set of kicker amplitudes after obtaining the calibrated model.

Figure 3b shows the turn-by-turn BPM data for the optimized single-mode injection, representing the end point of painting in the phase space, $\mathbf{K}_T$. The amplitude of mode two has been reduced in both planes, which can be seen in the reduced modulation of the envelope despite coupling in the lattice. The square of the amplitude of each mode is proportional to the emittance. Thus, the ratio of the amplitudes for sin-

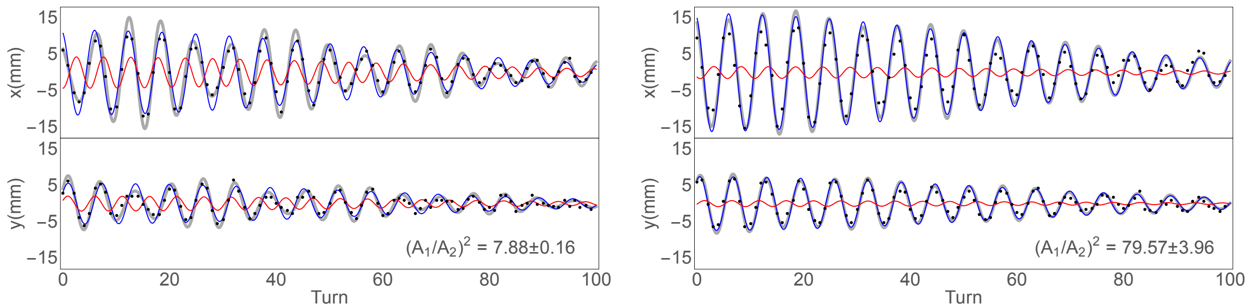

(a) Calibration Data

(b) Optimized Injection

FIG. 3. Turn-by-turn BPM data (black points) for tune calibration and optimized injection from location A10 in the ring injection straight showing the fit trajectory in gray and contributions from mode 1 (blue), mode 2 (red). Offsets have been removed.

gle particle injection sets an upper limit on the emittance ratio (or the minimal 4D volume) that can be achieved after painting. The maximum achievable emittance ratio based on a fit to the centroid of the injected beam is $(A_1/A_2)^2 \approx 80$. Ideally $A_2 \to 0$, but the ratio obtained here is large enough to suggest that control of the injection parameters does not significantly contribute to reduction in the final painted emittance ratio, which simulations predict to be ≈ 16 [13]. The difference between the single-particle amplitude ratio and the painted emittance ratio will be addressed later. The optimized injection in Fig. 3 corresponds to the coordinates $\mathbf{x}(t = T) = (10.3\text{ mm}, 0.03\text{ mrad}, 2.0\text{ mm}, 0.91\text{ mrad})$.

To inject onto the closed orbit at $t = 0$, we used a similar procedure to find $\mathbf{K}_0$, with the goal of minimizing both modes within the noise of the BPM's. With the kicker settings defined at the two end points, kicker waveforms were calculated according to Eq. 4 and used to inject 8.8 μC of beam over 600 turns.

We used the MENT algorithm [28] to reconstruct the accumulated 4D phase space distribution from 1D profile measurements of the extracted beam [29]. The reconstructed distribution, normalized to diagonalize the measured covariance matrix, is plotted in Fig. 4. According to the definition of the normalized coordinates, matched distributions should be axially-symmetric and their areas should correspond to the invariant emittances.

The RMS invariant emittances of the (u_1, u_1') and (u_2, u_2') distributions in Fig. 4 are 12.4 and 5.1 μm, respectively, giving a ratio of 2.4. This is about 7 times lower than the value of 16 demonstrated in best-case simulations. The discrepancy is due to the fact that these simulations assumed a larger final beam size than we were able to achieve.

An idealized Danilov distribution would be a uniformly-filled circle in the (u_1, u_1') phase space and a point in the (u_2, u_2') phase space. The difference in the size of distributions in the two modes in Fig. 4 indicates that beam was painted preferentially into one mode.

We model the painted distribution in (u_1, u_1') as a convolution of a 2D Gaussian of width σ_1 with a Heaviside

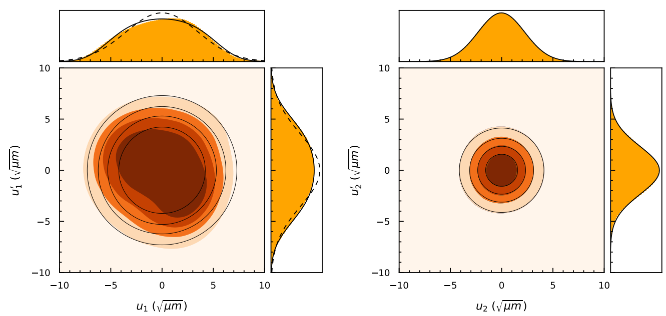

(a) Mode 1

(b) Mode 2

FIG. 4. 2D projections of the reconstructed 4D phase space distribution in normalized coordinates. Solid black lines indicate the contours and projection of the fit distribution. The dashed line in the projection shows a Gaussian distribution with equal RMS width to the fit for comparison.

step function in radius R:

$$\rho(\vec{u}_1|R, \sigma_1) = \int_{\vec{u}_1^{inj}} d^2\vec{u}_1^{inj} \frac{\Theta(1 - |\vec{u}_1^{inj}|/R)}{\pi R^2} \times \frac{1}{2\pi\sigma_1^2} \exp\left(-\frac{|\vec{u}_1 - \vec{u}_1^{inj}|^2}{2\sigma_1^2}\right) \tag{6}$$

Fitting to Eq. 6 gives, $\sigma_1 = 1.79 \pm 0.01\ \sqrt{\mu m}$ and $R = 6.03 \pm 0.01\ \sqrt{\mu m}$.

Assuming no painting in mode 2, we fit the (u_2, u_2') distribution with a simple 2D Gaussian giving a standard deviation, $\sigma_2 = 2.292 \pm 0.001\ \sqrt{\mu m}$.

Figure 4 shows contours for the fit functions in black, along with 1D projections onto the u, u' axes for each mode. In the left plot, the dotted line over the 1D projections indicates the projection of a 2D Gaussian with the same rms width as the data to contrast with the convolution.

In the presence of space charge, the eigenvectors of the matched beam are modified from the bare lattice values. Simulations showed that for the beam painted in these experiments the effect of space charge on the eigenvectors is small so we did not correct for them. The finite emittance of the linac beam, exacerbated by mismatch between the linac and ring optics, introduces non-linearities in the space charge that distort the beam during painting.

Ideally, the Gaussian widths squared $\sigma_1^2 = 3.20$ μm and $\sigma_2^2 = 5.25$ μm would match the injected emittances. However, they are larger than the direct contribution of the injected emittance of $\varepsilon^{inj} \approx 0.3$ μm. Using the previously measured linac optics parameters at the injection point and the periodic ring optics at the same point, we estimate that mismatch is responsible for an increase of a factor of ≈ 2 in the emittance in each plane (or $\approx \sqrt{2}$ in the Gaussian widths). Thus, mismatch explains a small portion of the difference. The rest of the difference can be attributed to collective and non-linear effects due to the non-negligible injected beam size relative to the final painted volume.

Conclusion—We have implemented uniform *eigenpainting*, a method to self-consistently paint a special case of the KV distribution in a coupled ring by predominantly filling one of its non-planar modes. We generated a beam with 4D emittance lower than an uncoupled beam with similar footprint in the x-y plane, achieving an emittance ratio of 2.4. We note that this is below the best value achieved in simulation of ≈ 16, but crosses the threshold for a reduction of the space charge tune shift relative to a planar beam [14].

We identified the following sources of error contributing to deviations from best-case simulations. The relative size of the injected beam to the final painted volume dominates. Mismatch between linac and ring optics, and modifications to the eigenvectors due to the effect of space charge on the matched solution also contribute. Imperfect control of the injection parameters to inject into the chosen mode is negligible.

Issues of beam size and matching do not represent a fundamental limit on the beam quality, only a limitation of the SNS configuration. From simulation we expect the effect of space charge on the orientation of the eigenvectors to be contribute only a small error in these experiments. However, the degree to which this effect can be accounted for during painting is an open question, and would likely set the fundamental limit on the quality of higher-intensity beams in purpose-built injection systems.

In the current SNS geometry excessive beam loss due to scattering in the foil would be a barrier to eigenpainting during normal operation because of the geometry of the injection region. This is not a fundamental limitation relative to standard injection schemes and could be addressed with a more suitable design, or eliminated completely with laser-based charge exchange [30].

The quality of uniformly eigenpainted beams after transport and acceleration, particularly as the assumption of a coasting beam becomes unreasonable, is uncertain. However, eigenpainting would still be useful if circular modes could be maintained with a non-uniform charge density. For instance, circular modes alone provide benefits related to space charge reduction, and flat beams for luminosity increase [4].

Finally, we note that eigenpainting beams with intense space charge near equilibrium offers a unique opportunity to study open questions related to high-intensity hadron beams. Particularly interesting are questions of halo formation, beam stability, and space charge reduction.

Acknowledgements—We would like to thank Charles Peters for help in the control room, and Sarah Cousineau for helpful feedback on this manuscript. We would also like to acknowledge Steve Lund for pointing out that the Danilov distribution is a special case of the KV. This manuscript has been authored by UT-Battelle, LLC, under contract DE-AC05-00OR22725 with the US Department of Energy (DOE). The US government retains and the publisher, by accepting the article for publication, acknowledges that the US government retains a nonexclusive, paid-up, irrevocable, worldwide license to publish or reproduce the published form of this manuscript, or allow others to do so, for US government purposes. DOE will provide public access to these results of federally sponsored research in accordance with the DOE Public Access Plan (https://www.energy.gov/doe-public-access-plan).

[1] D. W. Hudgings and A. J. Jason, "Injection system for the proton storage ring at lasl," in *11th International Conference on High-Energy Accelerators: Geneva, Switzerland, July 7–11, 1980*, edited by W. S. Newman (Birkhäuser Basel, Basel, 1980) pp. 277–282.

[2] V. Danilov, S. Cousineau, S. Henderson, and J. Holmes, Phys. Rev. ST Accel. Beams **6**, 094202 (2003).

[3] I. M. Kapchinskij and V. V. Vladimirskij, in *2nd International Conference on High-Energy Accelerators* (1959) pp. 274–287.

[4] A. Burov, Phys. Rev. ST Accel. Beams **16**, 061002 (2013).

[5] A. Oeftiger and O. Boine-Frankenheim, Phys. Rev. Lett. **132**, 175001 (2024).

[6] V. Danilov and S. Nagaitsev, Phys. Rev. ST Accel. Beams **13**, 084002 (2010).

[7] M. Chung, H. Qin, R. C. Davidson, L. Groening, and C. Xiao, Phys. Rev. Lett. **117**, 224801 (2016).

[8] S. M. Lund, T. Kikuchi, and R. C. Davidson, Phys. Rev. ST Accel. Beams **12**, 114801 (2009).

[9] E. Crosbie and K. Symon, Conf. Proc. C **950501**, 3167 (1996).

[10] I. Hoffman, L. Laslett, L. Smith, and I. Haber, Particle Accelerators **13**, 145 (1983).

[11] V. Danilov, S. Cousineau, S. Henderson, J. Holmes, and M. Plum, in *Proc. EPAC* (2004).

[12] V. A. Lebedev and S. A. Bogacz, Journal of Instrumentation **5**, P10010 (2010).

[13] J. A. Holmes, T. Gorlov, N. J. Evans, M. Plum, and S. Cousineau, Phys. Rev. Accel. Beams **21**, 124403

(2018).
[14] A. Burov, Y. Derbenev, and F. J. N. News, Submitted to Phys.Rev.Lett. (2009).
[15] A. Burov, S. Nagaitsev, and Y. Derbenev, Phys. Rev. E **66**, 016503 (2002).
[16] Y.-L. Cheon, S.-H. Moon, M. Chung, and D.-O. Jeon, Phys. Rev. Accel. Beams **25**, 064002 (2022).
[17] B. M. O. Gilanliogullari and P. Snopok, in English*Proc. IPAC'23*, IPAC'23 - 14th International Particle Accelerator Conference No. 14 (JACoW Publishing, Geneva, Switzerland, 2023) pp. 2391–2394.
[18] Y. S. Derbenev and A. Skrinskii, *Magnetization effects in electron cooling*, Tech. Rep. (AN SSSR, 1977).
[19] S. Nagaitsev, D. Broemmelsiek, A. Burov, K. Carlson, C. Gattuso, M. Hu, T. Kroc, L. Prost, S. Pruss, M. Sutherland, C. W. Schmidt, A. Shemyakin, V. Tupikov, A. Warner, G. Kazakevich, and S. Seletskiy, Phys. Rev. Lett. **96**, 044801 (2006).
[20] Y. Luo, D. Xu, M. Blaskiewicz, and C. Montag, Phys. Rev. Lett. **132**, 205001 (2024).
[21] Y. Kamiya, in *Proceedings of the 1989 IEEE Particle Accelerator Conference, . 'Accelerator Science and Technology* (1989) pp. 660–662 vol.1.
[22] J. Beebe-Wang, Y. Y. Lee, D. Raparia, and J. Wei, in english*Proc. PAC'99* (JACoW Publishing, Geneva, Switzerland) pp. 1743–1745.
[23] More exotic schemes have also been proposed with, e.g., anti-correlated painting sinusoidal variation in the action attempting to slowly build up space charge over the entire footprint, but this has never been demonstrated as it would lead to unacceptable beam loss [31]. This scheme could be revisited in light-based charge exchange.
[24] H. Hotchi, Phys. Rev. Accel. Beams **23**, 050401 (2020).
[25] A. Hoover, N. J. Evans, and J. A. Holmes, Phys. Rev. Accel. Beams **24**, 044201 (2021).
[26] Here we assume continuous injection of a point-like beam. In practice a finite beam size, and discrete injection will require some accounting for transient effects.
[27] T. Pelaia, II, arXiv.org Repository **2016** (2016).
[28] G. Minerbo, Computer Graphics and Image Processing **10**, 48 (1979).
[29] A. Hoover, Phys. Rev. Accel. Beams **27**, 122802 (2024).
[30] A. Aleksandrov, S. Cousineau, T. Gorlov, Y. Liu, A. Oguz, A. Shishlo, A. Zhukov, and M. Kay, Phys. Rev. Accel. Beams **26**, 043501 (2023).
[31] J. Beebe-Wang, *Oscillating Injection Painting And Related Technical Issues*, Tech. Rep. (BNL/SNS, 2000).